A Multibody Model of Federica Hand

Maria Yu. Karelina, Eduard Krylov, Cesare Rossi, Sergio Savino, Francesco Timpone

***Abstract* — The mechanical behavior of a recently patented mechanical hand is examined by means of a multibody model. The hand is an under-actuated and self-adapting system that was conceived as human hand prosthesis.**

Test results are also presented as an application example; they showed that both the proposed model and the technique can be very useful for the study of the considered mechanical system.

The research was carried on in cooperation among Italian and Russian Universities.

***Index Terms* —Tendon driven mechanism, Dynamical Simulation, Mechanical hand.**

I. Introduction

In the last decades robotics has largely drawn inspiration from biology, in particular, much attention has been made to replicate the hardware of the natural mechanisms.

One of the fields of robotics that has mainly taken inspiration from biology is the one relative to the gripper, in order to increase as much as possible the dexterity of these components.

In general, a robotic gripper can grasp in many different ways; the main distinction that is made is between a power grasp and a dexterous grasp.

The grasp of a human hand is always adapted to the type of task to perform and to the nature of the grasped object. For heavy objects or for delivering a large force a robust grasp is needed, while for lighter object a different and more dexterous grasp can be used. For these reasons research and industries focus their attention on developing robotic hands that "copy" the human hand.

One of the characteristic features in the evolution of robotic hands was the transition to the "underactuated" robotic hands which have a number of actuators lower than the number of degrees of freedom of the system.

Manuscript received February 11, 2016; revised July 25, 2016.

Maria Yu. Karelina is with The Moscow State Technical Automobile and Road University (MADI), Leningradskiy prosp., 64, 125319 Moscow, Russia (e-mail: *karelinamu@mail.ru*).

Eduard Krylov is with Kalashnikov Izhevsk State Technical University, Studencheskaya Str., 7, 426069 Izhevsk, Rus. (e-mail: *649526@mail.ru*).

Cesare Rossi is with Department of Industrial Engineering of University of Naples "Federico II", via Claudio n. 21, 80125, Naples, Italy (e-mail: cesare.rossi@unina.it).

Sergio Savino is with Department of Industrial Engineering of University of Naples "Federico II", via Claudio n. 21, 80125, Naples, Italy (e-mail: sergio.savino@fastwebnet.it).

Francesco Timpone is with Department of Industrial Engineering of University of Naples "Federico II", via Claudio n. 21, 80125, Naples, Italy (corresponding author: Francesco Timpone; phone: +39 081 76 83263; fax: +39 081 2394165; e-mail: francesco.timpone@unina.it).

The experimental prosthetic hand presented by Dechev at al., 2001, [1], is able to perform passive adaptive grasp, that is, the ability of the fingers to conform to the shape of an object held within the hand.

Brown and Asada, 2007, [2], collected a variety of human hand postures and used the principal components analysis to calculate the synergies between fingers, they called "eigenpostures" these hand postures. They presented a novel mechanism design to combine the eigenpostures and drive a 17-degree-of-freedom 5-fingered robot hand using only 2 DC motors.

Gosselin et al., 2008, [3], presented the design and experimental validation of an anthropomorphic underactuated robotic hand with 15 degrees of freedom and a single actuator.

Catalano et al., 2012, [4], presented the first implementation of the UNIPI-hand, a prototype which conciliates the idea of adaptive synergies for actuation with an high degree of integration, in a humanoid shape.

Many mechanical systems used for grasping devices have been conceived with multi finger systems that work likewise the human hand, [7-12], or even consist in human prostheses, and in this fields, many studies were carried out to reduce the cost and the development time, [13-15]. In the grasping devices that use fingers, if the system's dimensions are comparable to those of an human hand, it is rather difficult to operate each of the finger phalanxes by a (micro) motor, so the fingers are moved by tendons. The latter can be elastic, [3-6], or inextensible. Elastic tendons essentially permit to obtain a system that is easier to be operated and that can easily permit to each finger to adapt its bending to the shape of the object during the grabbing even if a single actuator for all the fingers is used. On the other side, inextensible tendons conceptually permit to exert ah higher grasping force but generally, if different bending of the finger are required, more complex actuator systems are required.

Finally, the kinematic pairs between the phalanxes can be made up by simple hinges of more complex joints like the Hillberry's rolling Joint, [4].

It is well-known that in human hands and animal paws in general, each finger has two different (almost inextensible) tendons to be bended and each tendon has his own actuator.

The present paper concerns a model of a single tendon three phalanges finger that is used in a multi- finger grasping device. By means of this finger and a differential system, it is possible to use one only actuator to move all the fingers of the hand, [14-17]. The grasp is always adapted to the shape of grasped object, and each finger grasps the object with the designed force.

II. Federica Hand model

A 3D model of a 5-fingered hand (Fig. 1) has been developed and the working schemes of this hand model (Fig.2) and of the finger (Fig. 3) are reported. It is possible to change the geometric parameters of all phalanges (and all fingers) in a dialog window (Fig.4). The hand scheme consists of 5 "finger" blocks with "Rigid Transform" blocks (Fig. 2) able to locate them with respect to each other (Fig. 1).

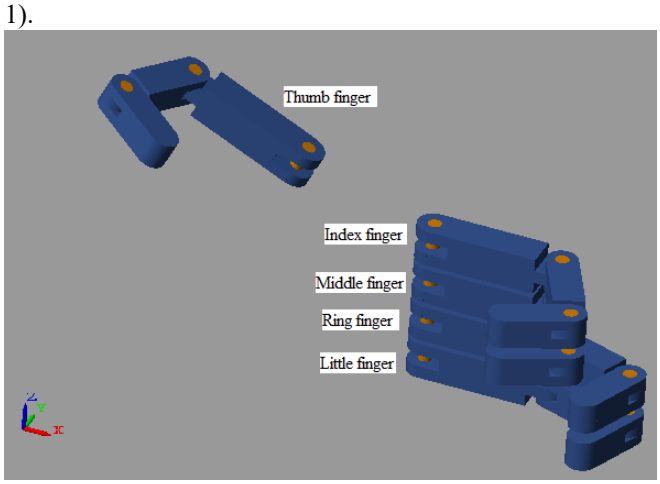

Fig. 1. Federica Hand 3D model

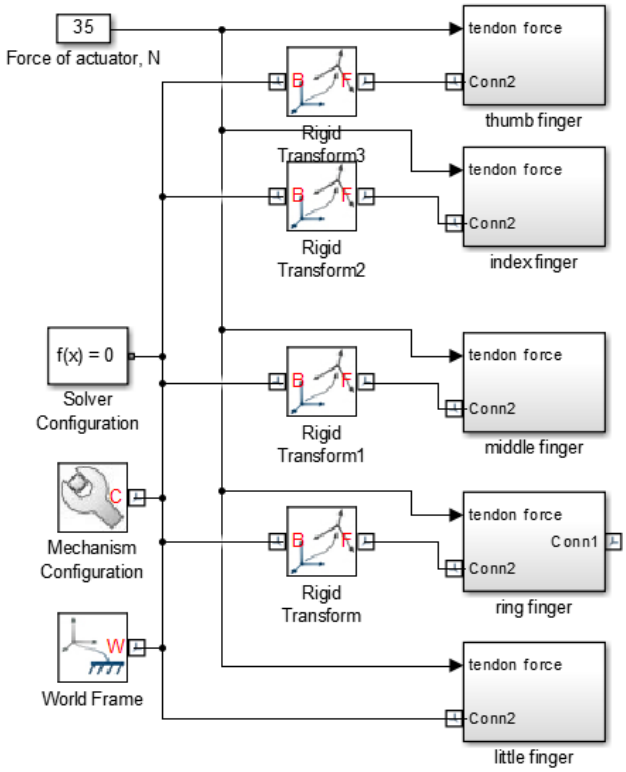

Fig. 2. The working scheme of hand model

In order to simulate the presence of tendons inside the fingers, distributed forces have been applied (Fig. 5). Force of actuator (Fa) in Newtons (Fig. 2) is the main input and it will be automatically distributed for the 5 fingers, respectively, Fa/4 – thumb, index, middle fingers; Fa/8 – ring, little fingers (Fig. 3, tendon force, Fa/8). To close all fingers a minimal actuator's force Fa = 5 N is necessary, when gravity in Y direction of "World Frame" (perpendicular to palm) is active (Fig. 6, gravity).

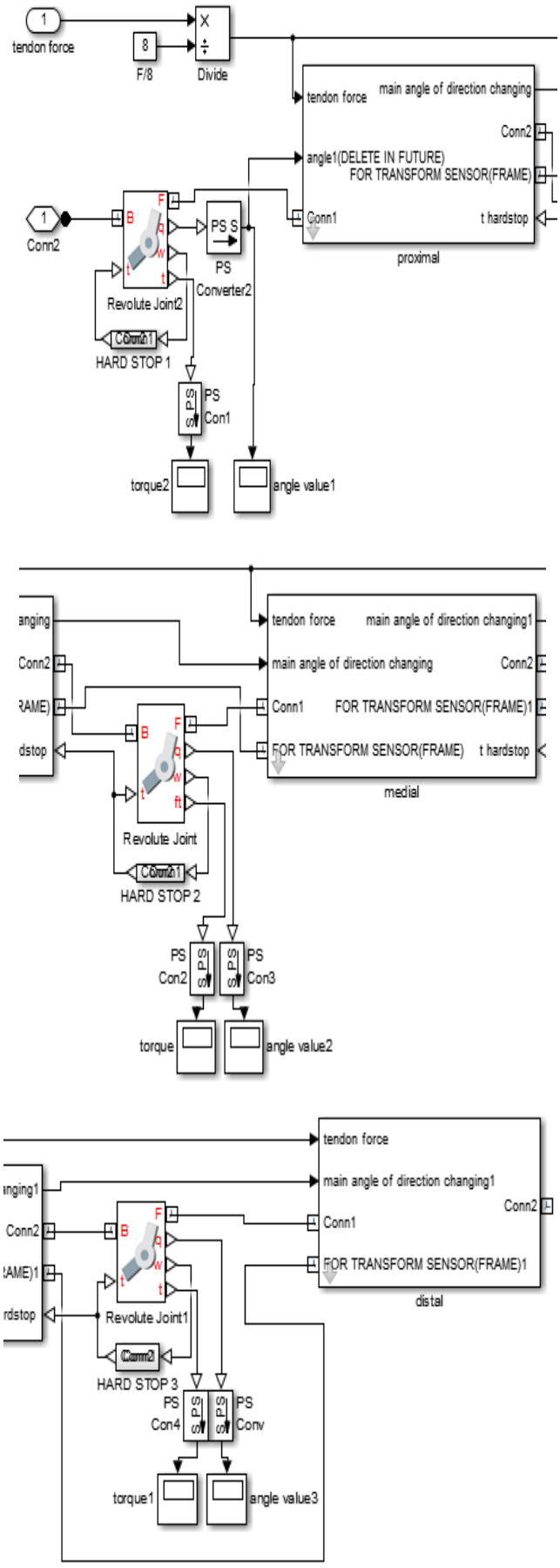

Fig. 3. The working scheme of little finger model

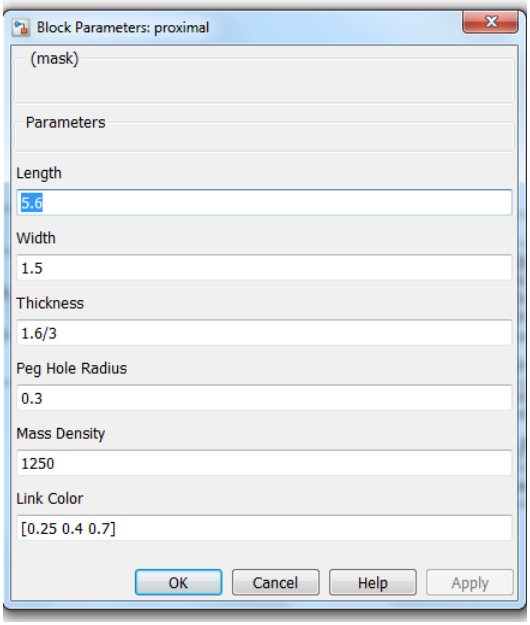

Fig. 4. Dialog window of "Proximal" subsystem parameters

In the model the following assumptions have been adopted: absence of friction phenomena, replacement of the tendon with a constant repartition of forces.

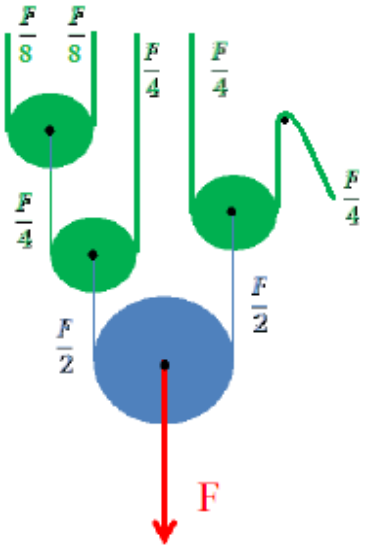

Fig. 5. Force distribution among fingers

III. Finger Model Structure

Input parameters of each phalanx (Fig. 6) are: length (L), width (W), thickness (T), peg-hole radius (R), mass density, link color.

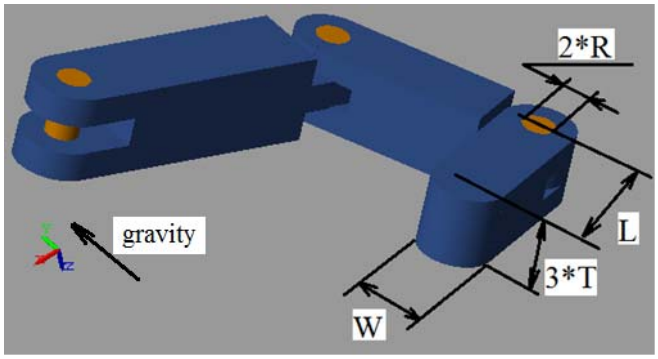

Fig. 6. Parameters of phalanx

To create the shape of the joint in this phalanx (hole and peg) 3 bodies have been rigidly connected (Fig. 7, blue highlight) with thickness (T). So, thickness of phalanx is equal to (3*T) three multiplied to Thickness (T) (Fig. 6, Thickness parameter). The scheme of each finger (Fig. 3) consists of three main subsystems: "proximal", "medial", "distal", three "hard stops" and main blocks, three "revolute joints" and blocks for output angles and torque values (Fig. 8, torque, angle value2). It is also possible to output other characteristics of moving as for example: angular velocity, angular acceleration and so on.

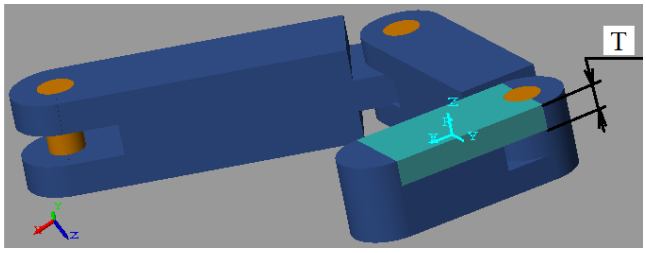

Fig. 7. Part of phalanx

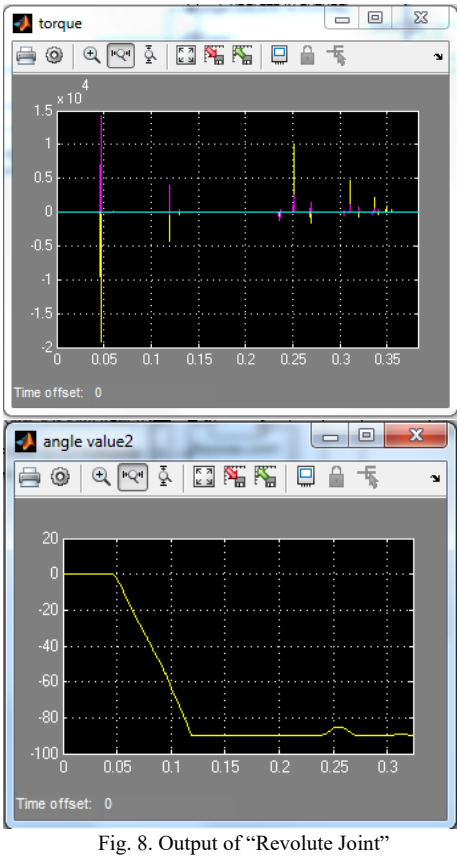

Fig. 8. Output of "Revolute Joint"

The basis of the model consists of "Rigid Transform" blocks and "Revolute Joint" blocks. Consider, for example, medial phalanx, that is connected on both sides by means of "revolute joint" and "revolute joint1", respectively, using entrances "Conn1" and "Conn2" (Fig. 3). Also these "Conn1" and "Conn2" are connected with the basis of phalanx inside subsystem "medial" (Fig. 15) by means of "rigid transform" blocks. Each "rigid transform" block represents a rigid roto-translation between two reference systems. To create a body a "Solid" block has been used and

it has been connected to a “rigid transform” block to set the location of the body.

Subsystems “Hard stop” are located under each “Revolute Joint” block and contain (Fig. 10 a) a “Rotational Hard Stop” block. Universal Parameters of “Rotational Hard Stop” for all “Revolute Joints” blocks are shown in fig. 11. “Upper bound” and “Lower bound” allow to set up the excursion range of a “Revolute Joint” (they can be set in the window properties of Revolute Joint).

“Hard stop” block works with parameters of “Revolute Joint” block (Fig.10, b): Input torque (t) and sensing velocity (w) (angular velocity). When distal phalanx reaches its “lower bound” (Fig.9), “hard stop” block applies a torque to the revolute joint of distal phalanx to stop rotation, but it is also necessary to apply an opposite torque to the medial phalanx. In the real prototype, instead of torque of “Hard stop” and opposite torque (to medial phalanx) there is (fig. 9) the contact force acting on the distal (Fc.d) phalanx and the opposite of the contact force (Fc.m), acting on the medial phalanx (Fc.d = -Fc.m). The opposite torque on the medial phalanx is equal to Fc.m* Arm. In the model the opposite of the torque acts towards the medial phalanx inside subsystem “medial” (Fig. 15, “t hardstop”) by means of the input “t hard stop” (fig. 10,b) and is equal to torque of Hard Stop.

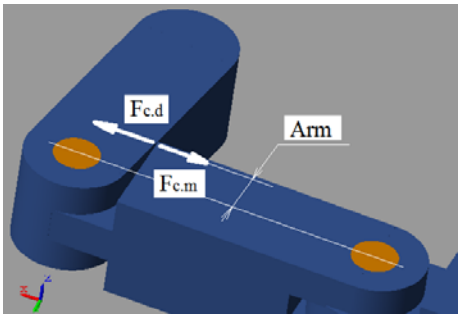

Fig. 9. Opposite forces, acting on 2 different phalanges

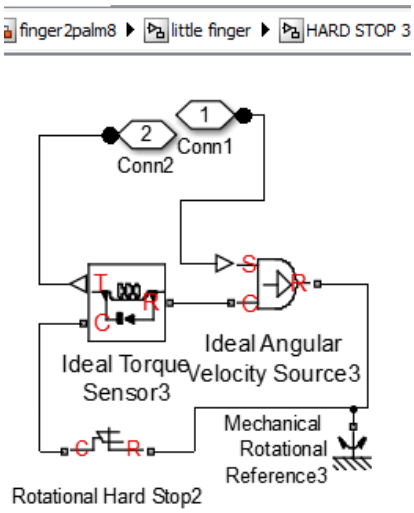

a)

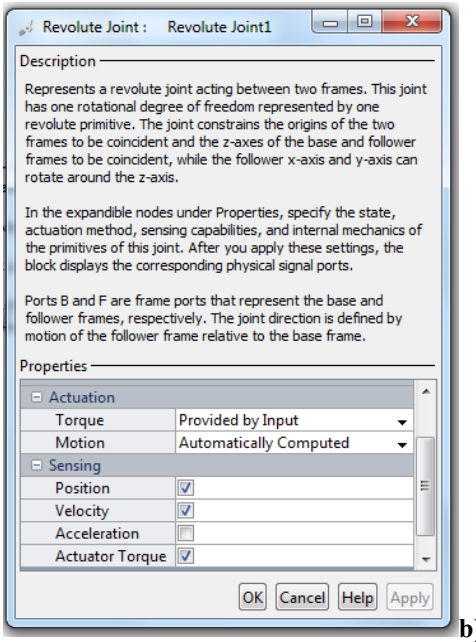

b)

Fig. 10. a) Inside “Hard Stop” subsystem; b) Parameters of “Revolute Joint” blocks

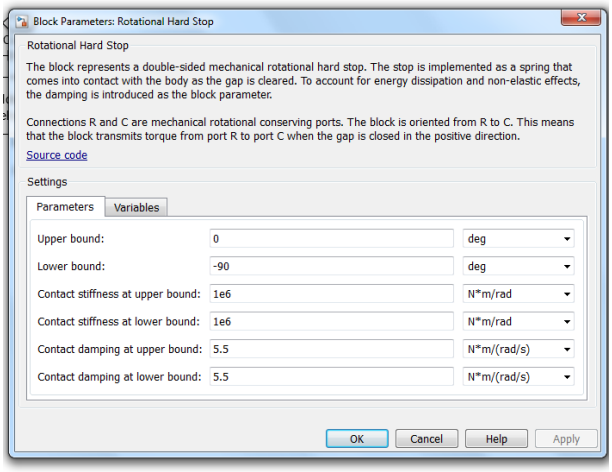

Fig. 11. Parameters of “Rotational Hard Stop” block

IV. Working Scheme of Distal Phalanx

The body of phalanx consists of “Solid” blocks (Fig. 12, “Peg”, “HoleA”, “Main Side1”, “Hole B”, and so on) with different shapes, dimensions and locations in space. As said the position of “Solid” blocks can be set by means of by “Rigid Transform” blocks (Fig. 12, “for Hole A1”, “for main side2” and so on). Also “Rigid Transform” blocks (Fig. 12) have been created “for force1” (Fig. 13: a) and “for force2” (Fig. 13: a), for attachment forces of the tendon along X and Y directions (Fig. 12, “External Force and Torque2,3”). If the tendon does not act along the center-line of phalanx (and also not along the X axis “for force2”, because the phalanx is parallel to the X axis “for force”), there will be also an Fy component of Force.

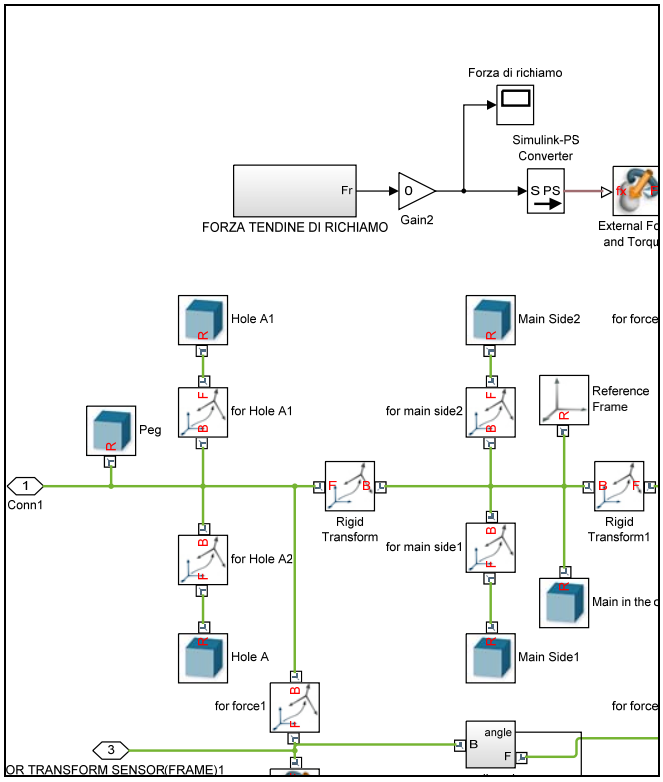

a)

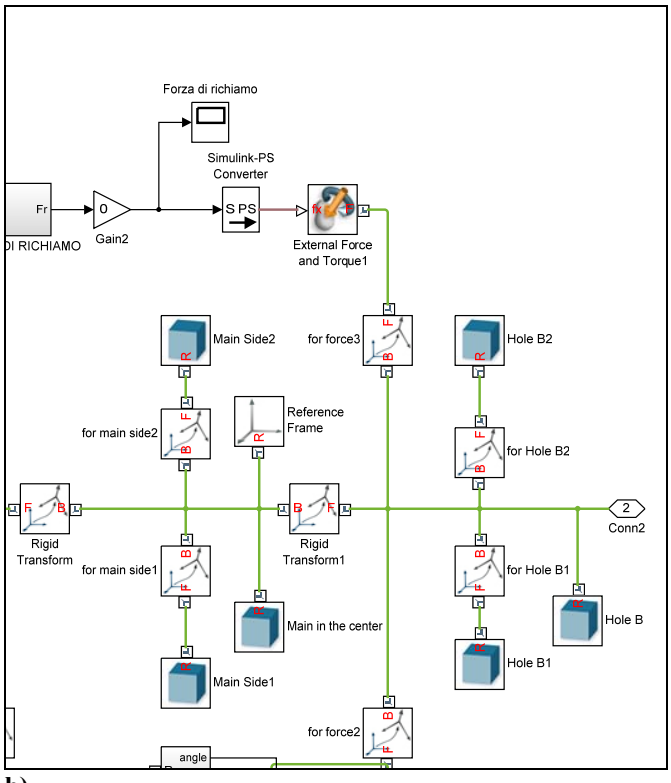

b)

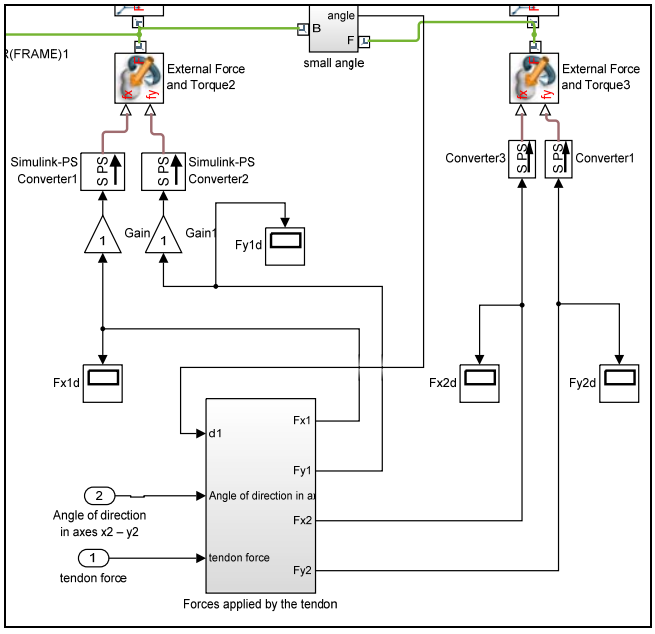

c)

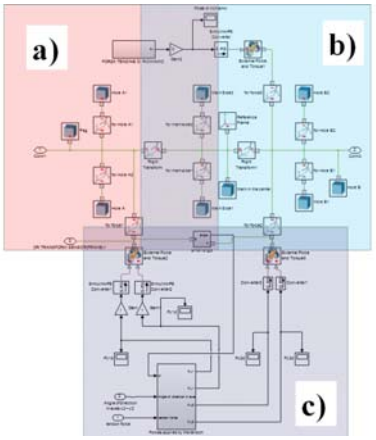

Fig. 12. Working scheme of the distal phalanx

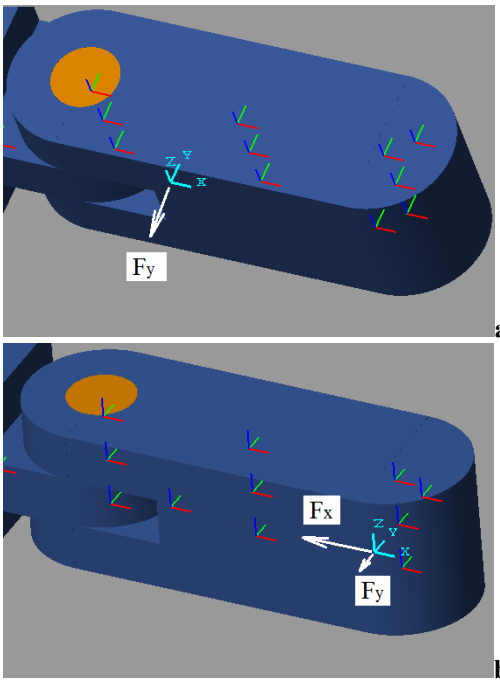

a)

b)

Fig. 13. a) Forces of tendon in point “for force1”; b) Forces on tendon in point “for force2”

In figure 14 it is possible to distinguish:

A – point of connection of the body of the distal phalanx to the tendon (point of frame "for force2");

B – point of tendon sliding by the distal phalanx (point of frame "for force1").

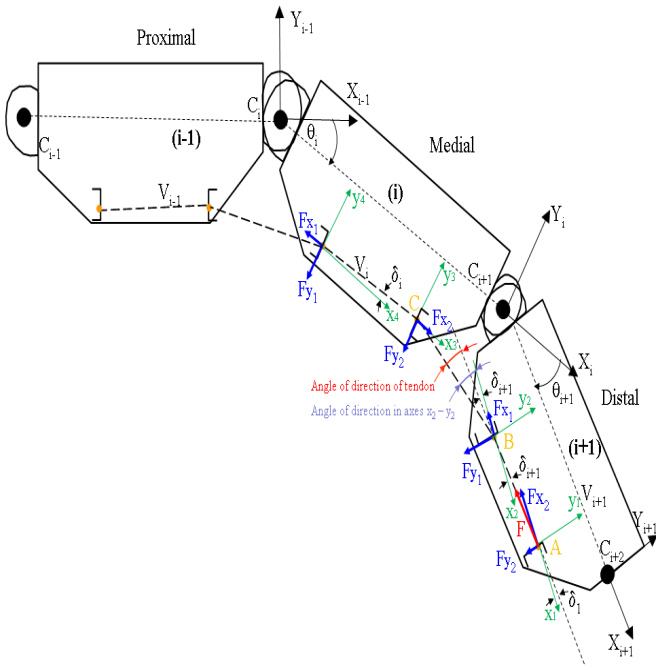

Fig. 14. Calculation scheme of distal phalanx angles

The tendon forces acting on the distal phalanx have been considered in the reference frames "for forces" – points (Fig. 14, points A, B). Directions x1 and x2 in the frames (x_1 - y_1) and (x_2 – y_2) are parallel to the distal phalanx (C_{i+1}, C_{i+2}) and not parallel to tendon AB (tendon can be parallel to the phalanx and $x_{1,2}$ direction, if x_1 and x_2 are located on one line).

δ_1 – small constant angle, depending on reference locations of points A and B.

By a "Transform Sensor" block (Fig. 12) between "for force1" and "for force2" it is possible to calculate angle δ_1 and see its value in "d1 value" block. So, if coordinates of points A and B will be changed, angle δ_1 will be automatically recalculated.

F – force applied to the distal phalanx by tendon in the connecting point (point A). F acts along the tendon and it is equal to internal force inside the tendon (-F), but in the opposite direction.

In the middle of the scheme (Fig. 12) it is possible to see the blocks: "External Force and Torque2" and "External Force and Torque3", that apply the actions of the tendon. The force that these blocks apply are described by following relation.

[Angle of direction of tendon] = (Angle of direction in axes x2 – y2) - δ_i (1)

Fx1 = -|F| * cos ([Angle of direction of tendon]) (2)

Fy1 = -|F| * sin ([Angle of direction of tendon]) (3)

Fx2 = -|F| * cos(δ_1) (4)

Fy2 = -|F| * sin(δ_1) (5)

V. Working Scheme of the Medial Phalanx

There are some differences in schemes between the medial and the distal phalanx.

"Medial" subsystem (phalanx):

1. Has opposite "hard stop" torque (is equal to "Hard stop" block's torque) from the entrance "t hardstop"

2. Has "transform sensor3" (Fig. 12) to measure the angle of point C regarding to (x_2 – y_2) and "transform sensor4" to measure the angle of point B regarding to (x_3 – y_3) .(Fig. 16, Angle of direction in axis x_3 – y_3).

3. Transform sensor determines the relative position by connecting with point C (Fig.15, "for force2") and point B by entrance "for transform sensor(frame)1" in the "distal". (Fig.12, "for force1").

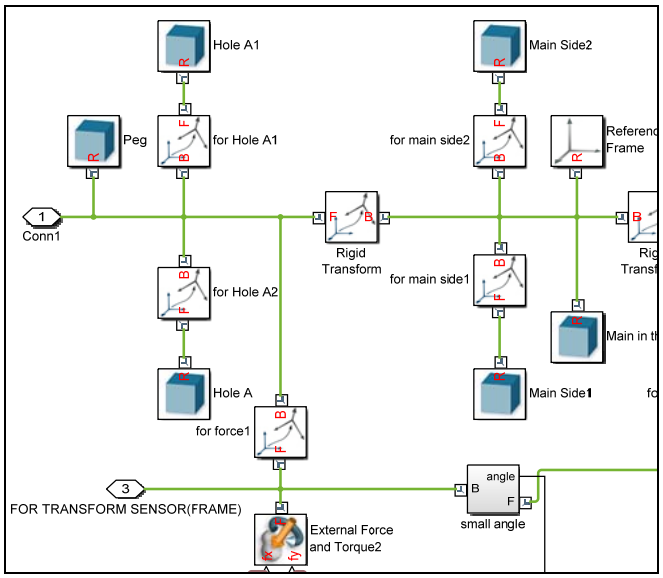

a)

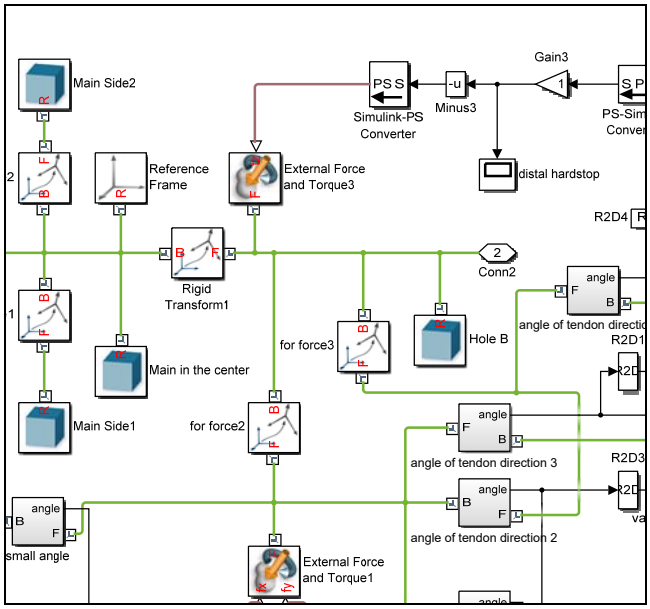

b)

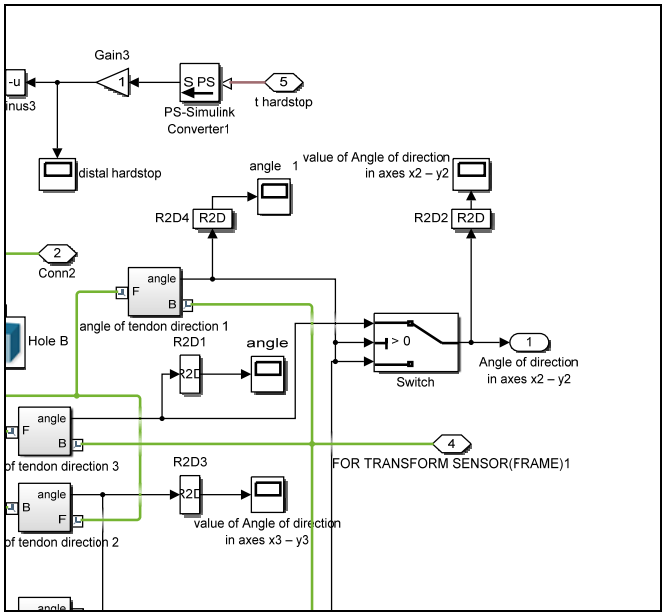

c)

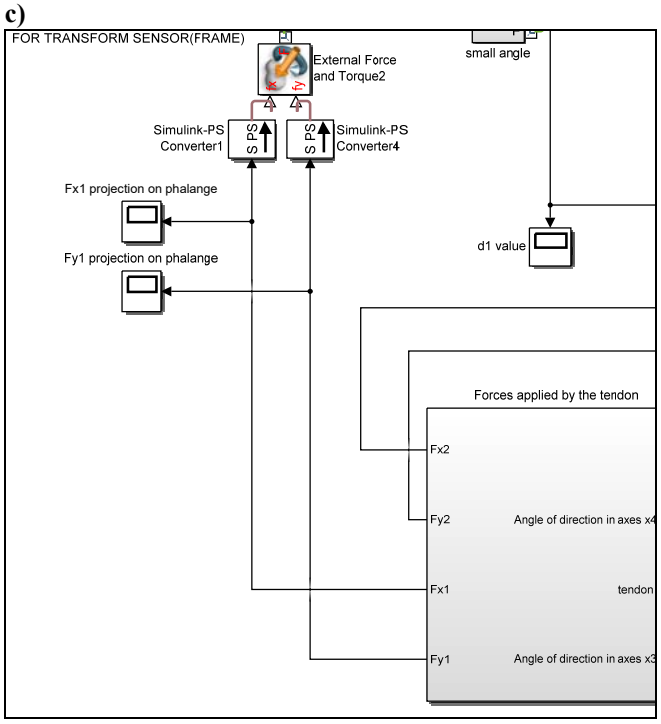

d)

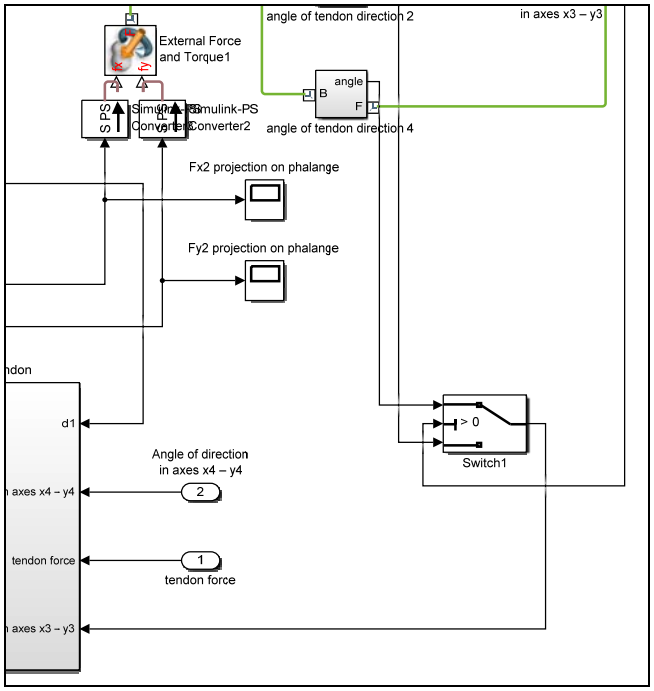

e)

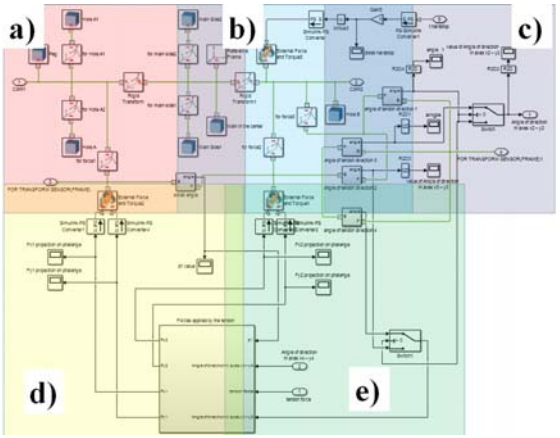

Fig. 15. Working scheme of the medial phalanx

In the middle of the scheme (Fig. 15 a), b)) it is possible to see the blocks: “External Force and Torque2” and “External Force and Torque1”, that apply the actions of the tendon. The force that these blocks apply are described by the following relation.

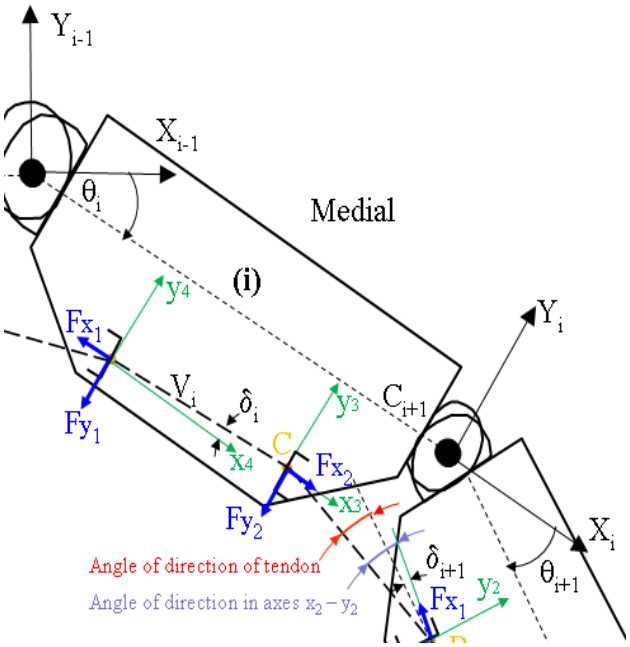

Fig. 16. Calculation scheme of the medial phalanx angles

[Angle of direction of tendon 2] = ((Angle of direction in axes $x_3 - y_3$) + ($-\delta_2$)) (6)

$Fx_1 = -|F| * \cos([\text{Angle of direction in axes } x_4 - y_4] + \delta_2)$ (7)

$Fy_1 = -|F| * \sin([\text{Angle of direction in axes } x_4 - y_4] + \delta_2)$ (8)

$Fx_2 = |F| * \cos [\text{Angle of direction of tendon 2}]$ (9)

$Fy_2 = |F| * \sin [\text{Angle of direction of tendon 2}]$ (10)

VI. V.Working Scheme of the Proximal Phalanx

The working scheme of proximal phalanx is very similar to medial phalanx one, the only difference is in the first output of the guide of the tendon. For this phalanx the tendon comes out of the front surface and not from the lateral one, as seen in the scheme of Figure 17, in which the arrow indicates the further reference system associated with the exit point of the tendon.

In this way it is possible to increase the torque that the action of the tendon generates on the proximal phalanx.

For the actions that the tendon exerts on the phalanx, it is possible to do similar considerations to those made for the medial phalanx.

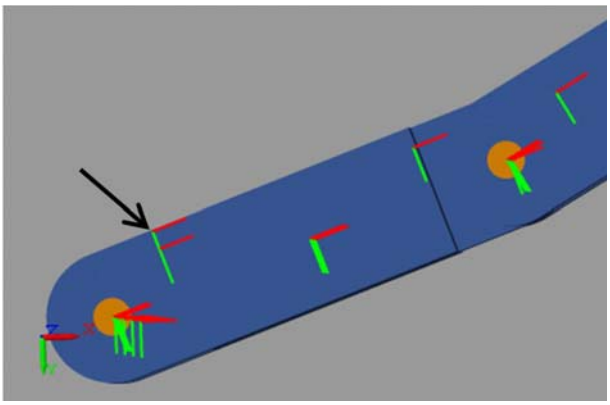

Fig. 17. Scheme of the proximal phalanx

VII. One Finger Model Simulations

A single finger simulation has been conducted in different conditions with the aim is to find out how its behavior depends on geometrical parameters, in particular, on position of tendon guides. In the following the results of 3 tests, in which the above parameters have been changed to observe the dynamical behavior of the finger, are reported.

The gravity has the same direction of Y axis of "World Frame" (Fig. 18).

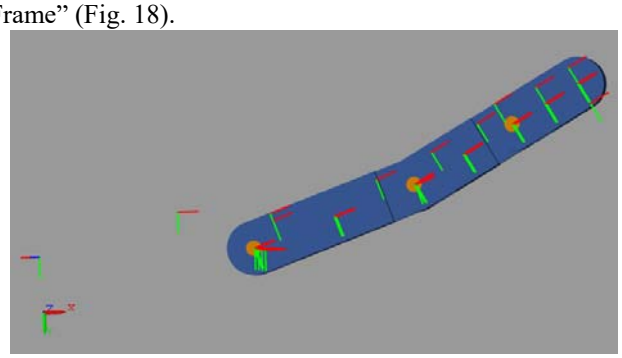

Fig. 18. Location of axis in the finger model for test 1

In the first two tests, the actuator force, is kept constant to 5N. This means that the tendon pulls with the same constant force during all the simulation, after an initial interval of 0.02 seconds, needed to reach the nominal value. In the third test the action of a motor that pulls the tendon is simulated. In this case the motor operates a displacement of the tendon and its control generates a traction force that is not constant.

Test 1. Tendon distance from hinges equal for three phalanges

In this first test the distance from the joints along the Y axis, of the tendon guide in all the phalanges is the same and it is equal to 5mm.

In figure 19 are shown the results of the test 1.

It is possible to observe that the first phalanx that reaches its final position (-90 degree), is the distal, whose angle of rotation is teta3; then the medial phalanx reaches its final position (angle teta2) and, finally, the proximal phalanx reaches in final position. A such closing sequence of the phalanges of the finger, is not preferable in grasping tasks, in fact with this sequence the finger closes on itself and is not capable of grasping any object.

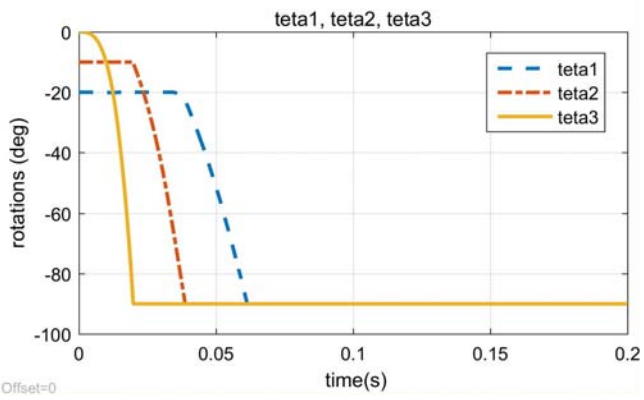

Fig. 19. Results of test 1 – Rotations of phalanges

Test 2. Tendon distance from hinges different for

three phalanges

In this second test the distances of the tendon guides are chosen different for each phalanx, as it is possible to see in figure 20.

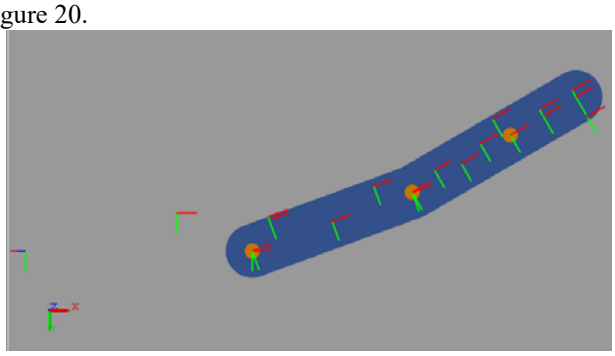

Fig. 20. Location of axis in the finger model for test 2

In figure 21 are shown the results of the test 2.

In this second test the closing sequence of the finger is different and, in particular, the proximal phalanx is the first phalanx to reach its final position, then the medial phalanx reaches its final position and finally the distal phalanx closes. This second kind of closing sequence is more advantageous in grasping task, in fact in this way the finger wraps around objects to grasp.

It is also evident that the total time to complete finger closing in the second test (0.04 seconds) is minor than the one of the first test (0.06 seconds), this happens because the change in the parameters, implies a change in the dynamical beaviour of the finger.

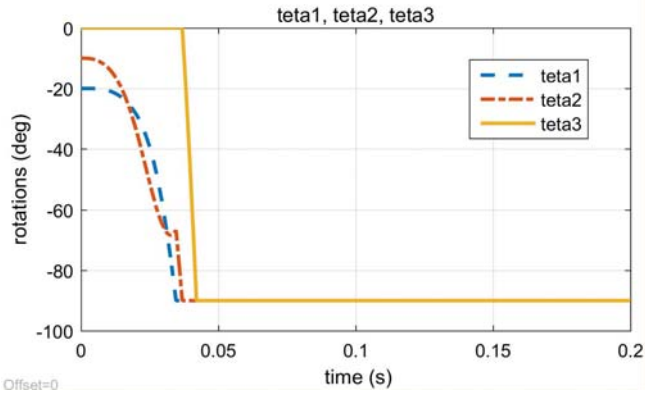

Fig. 21. Results of test 2 – Rotations of phalanges

The results of Test 2, clearly show that the finger behavior depends on its geometrical parameters, and so it is possible to identify the optimal configurations to set up the correct closing order of phalanges in order to grasp objects using this 3D model.

Test 3. Control of the displacement of the actuator tendon.

In the third test, the rules for implementing the traction force have been changed. It was assumed that the tendon is moved by a motor, in this case the motor is actuated to obtain a determined displacement of the actuator tendon, figure 22.

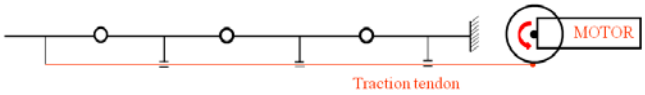

Fig. 22. Scheme of the finger with motor actuation

Such type of movements, generates a traction force very different from the one assumed constant in the previous tests.

In particular in Figure 23 it is possible to observe the behavior of the traction force of the tendon in the two cases: a) constant traction force, b) traction force for a given displacement of the tendon.

It is possible to observe that the residual traction force, after the finger is completely closed, in the two above cases is different. In fact, when the tendon applies a constant force, the residual traction force value is equal to the constant force, while, when the tendon is moved by a motor, the residual force depends on the difference between desired displacement and the final displacement of the tendon. The greater this difference, the greater the force with which the motor pulls the tendon to make him to achieve the desired displacement.

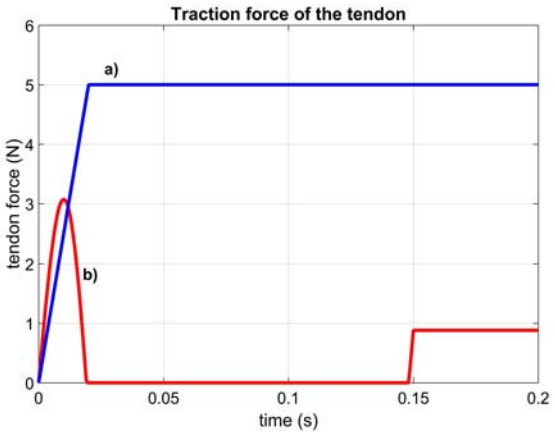

Fig. 23. Tendon traction force: a) constant traction force; b) traction force for a given displacement of tendon.

In figure 24 are shown the rotation angles of the finger during the simulation test 3.

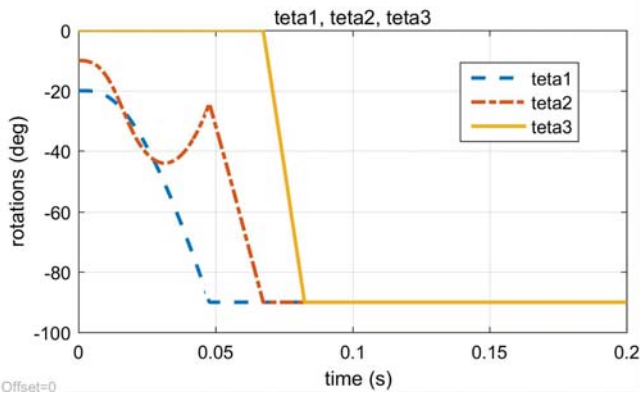

Fig. 24. Results of test 3 – Rotations of phalanges

Also in this third test the closing sequence of the finger is proximal-medial-distal. The dynamical behavior of the finger is changed again and the time to close the finger is bigger because the applied tendon traction force is

decreased respect to the constant value applied in the first two tests. By actuating the motor to obtain the desired tendon displacement, it is possible to observe a max value of the tendon force of 3 N (Fig. 23).

A more realistic simulation must provide for the presence of the antagonist tendon. The antagonist tendon opposites to the traction tendon action and allows to restore the finger in ex-tended configuration, figure 25. This tendon is fixed to the last phalanx, the distal one, and it flows in guides positioned on the upper side of the finger. The medial phalanx and the proximal phalanx terminate with a pulley on which the antagonist tendon wraps itself. So, the actions that the antagonist tendon generates on the phalanges are different for the distal phalanx and for the medial and proximal phalanx.

On the distal phalanx the action of antagonist tendon has the direction x and a value FR, and its point of application is the tendon attachment point, figure 8. On the medial and proximal phalanges the action of the antagonist tendon has a direction that depends on the rotation angle of successive phalanx and its point of application is in the hinge of the successive phalanx, figure 8. In equation (1) the antagonist tendon actions on the three phalanges are reported.

$$\begin{aligned} F_{A3x} &= FR;\ F_{A3y} = 0 \\ F_{A2x} &= FR(1-\cos\theta_3);\ F_{A2y} = FR\sin\theta_3 \\ F_{A1x} &= FR(1-\cos\theta_2);\ F_{A1y} = FR\sin\theta_2 \end{aligned} \quad (11)$$

Where:

F_{Aix} component of the action of the antagonist tendon on phalanx i in direction x;

F_{Aiy} component of the action of the antagonist tendon on phalanx i in direction y;

θ_i rotation angle of phalanx (i);

FR action of antagonist tendon.

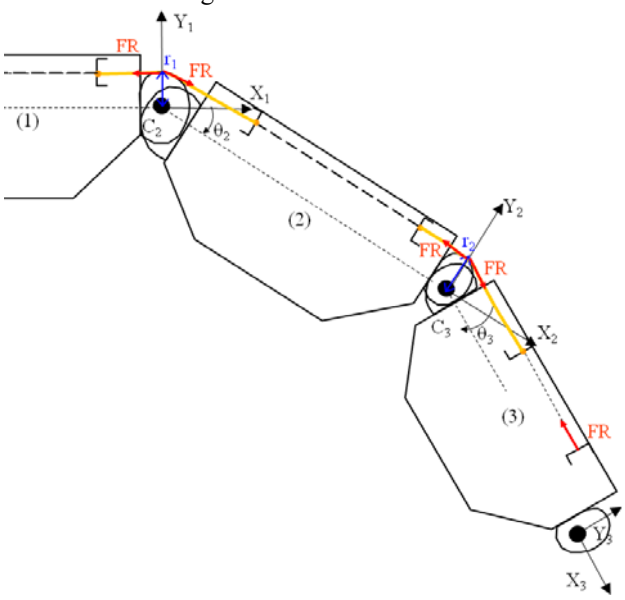

Fig. 25. Actions of antagonist tendon.

In the simplest case, the action of the antagonist tendon, FR, is implemented by a spring element with a stiffness k. In figure 26 a scheme of the actuation of the finger is shown.

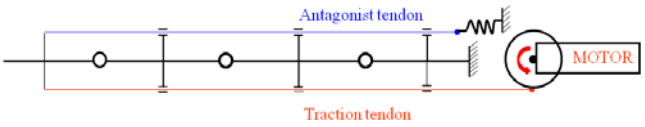

Fig. 26. Scheme of finger with antagonist tendon linked to spring element

In this modelling case, the actuator pulls the traction tendon with the same law of motion of free simulation, while a spring element pulls the antagonist tendon.

The action of traction tendon must always contrast the action of antagonist tendon.

In figure 27 the rotation angles of the three phalanges are shown for three different simulations in which the stiffness of the spring element of the antagonist tendon varies. In all three the simulations, the law of motion of the motor ensures a displacement ramp of the actuator tendon of 30 mm in 0.5 seconds.

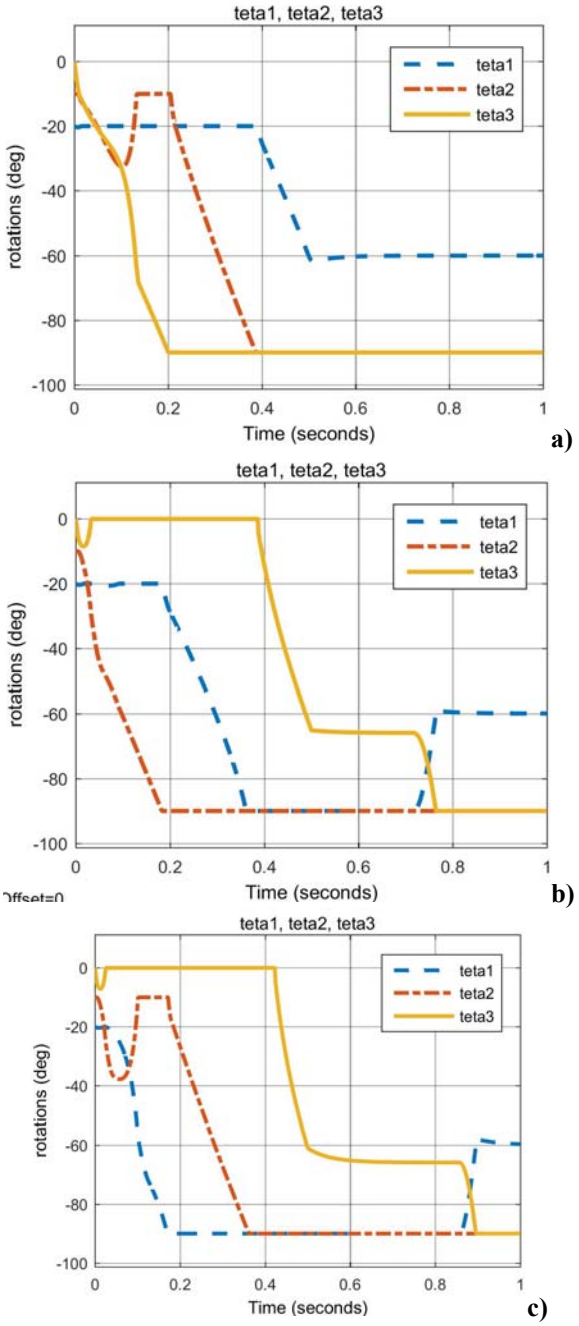

Fig. 27. Rotation angles of the three phalanges in simulations with antagonist tendon with fixed spring element: a) stiffness k=1.1 N/mm, b) k=2.5 N/mm, c) k=3.5 N/mm.

In figure 27a) k=1.1 N/mm and the closing sequence of the finger is "distal-medial-proximal". In-creasing the stiffness k the closing sequence of the finger changes, with k = 2.5 N/mm becomes "medial-proximal-distal", figure 27b), and with k = 3.5 N/mm is "proximal-medial-distal", figure 27c). With this type of antagonist tendon, the actuator tendon must always exert a force to keep the finger closed, like it is possible to observe in figure 28.

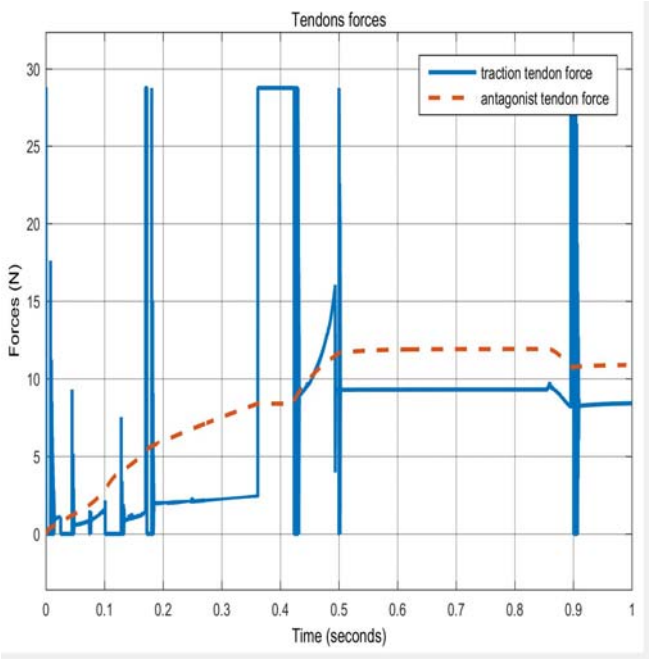

Fig. 28. Forces exert by tendons in simulations with antagonist tendon with fixed spring element with stiffness k=3.5 N/mm.

The diagram of figure 28 shows the force exerted by traction tendon and by antagonist tendon when the spring element has a stiffness k=3.5 N/mm. It is possible to observe that the antagonist tendon always exerts a force which is increasing with the displacement of the tendon itself, simultaneously, the actuator tendon can never cancel its action even when the final configuration of the finger has been reached.

This last test show that, in the behavior of the finger, and consequently of the entire hand, the application of the tendon force is a key parameter. The study of the law of motion with which the motor pulls the tendon is, therefore, a necessary step in the development of the mechanical hand. For this purpose, the model developed, is a very useful tool.

VIII. Conclusions

A multibody model of a recently patented mechanical hand has been proposed. The tests presented as examples show some aspects of the hand mechanical behavior and also that both the proposed model and the technique can be very useful for the study of the considered mechanical system. This mainly as far as the influence of some geometrical parameters is concerned.

What above suggests that the model can be usefully adopted to investigate on some aspects concerned with this hand prostheses as:

- the dynamical behavior of the fingers phalanxes before the contact with an object;
- the static behavior of the phalanxes once the gripping occurred;
- the appropriate law of motion to pull the tendon and to generate a dynamic behavior suitable for the gripping of the objects.

The aspects above are very important being the mechanism an under-actuated and self-adapting system.

The research was carried on in the context of a cooperation among Italian and Russian Universities and encourages further cooperation among them.

References

[1] Dechev N., W.L. Cleghorn, S. Naumann. 2001. *Multiple finger, passive adaptive grasp prosthetic hand*, Mechanism and Machine Theory, vol. 36, pp 1157-1173.

[2] Brown C. Y. and H. H. Asada. 2007. *Inter-Finger Coordination and Postural Synergies in Robot Hands via Mechanical Implementation of Principal Components Analysis.* In Proc. Of the 2007 IEEE/RSJ International Conference on Intelligent Robots and Systems, San Diego (CA, USA), October 29 - November 2.

[3] Gosselin C., F.Pelletier and T. Laliberté. 2008. *An Anthropomorphic Underactuated Robotic Hand with 15 Dofs and a Single Actuator*. In Proc. of 2008 IEEE International Conference on Robotics and Automation, Pasadena (CA, USA), May 19-23.

[4] Catalano M. G., G.Grioli, A. Serio, E. Farnioli, C. Piazza and A. Bicchi. 2012. *Adaptive Synergies for a Humanoid Robot Hand*. In Proc. of IEEE-RAS International Conference on Humanoid Robots, Osaka (Japan), October 2012.

[5] A. Bicchi, *Hands for Dexterous Manipulation and Robust Grasping: A Difficult Road Toward Simplicity*, IEEE TRANSACTIONS ON ROBOTICS AND AUTOMATION, 2000, Vol. 16, n. 6.

[6] F. Lotti, G. Vasura, *Design aspects for advanced robot hands*, In Proc.2002 IEEE/RSJ International Conference on Intelligent Robots and Systems, Lausanne, Switzerland, september 30 - October 4, 2002.

[7] Giorgio Grioli, Manuel Catalano, Emanuele Silvestri, Simone Tono and Antonio Bicchi, *Adaptive Synergies: an approach to the design of under-actuated robotic hands*, IEEE/RSJ International Conference on Intelligent Robots and Systems, 7-12 Oct. 2012.

[8] S. Roccella, M.C. Carrozza, G. Cappiello, P.Dario, J.J. Cabibihan, M. Zecca, H. Miwa, K. Itoh, M. Matsumoto, A. Takanishi, *Design, fabrication and preliminary results of a Novel anthropomorphic hand for humanoid robotics: RCH- 1*, Proceedings of 2004 IEEE/RSJ International Conference on Intelligent Robots and Systems, Sendai, Japan, September 28 - October 2, 2004.

[9] S. Roccella; M.C. Carrozza; G. Cappiello; J.J. Cabibihan; C. Laschi; P. Dario; H. Takanobu; M. Matsumoto; H. Miwa; K. Itoh; A. Takanishi, *Design and Development of Five-Fingered Hands for a Humanoid Emotion Expression Robot*, International Journal Of Humanoid Robotics, 2007, n. 4, pp. 181-206.

[10] S. Roccella, E. Cattin, N. Vitiello, F. Giovacchini, A. Chiri, F. Vecchi, M.C. Carrozza, *Design of a hand exoskeleton (handexos) for the rehabilitation of the hand*, Gerontechnology; N. 7(2), 2008, pp. 197:197.

[11] H. Yussof, M. Ohka, H. Suzuki, N. Morisawa, and J. Takata, "*Tactile sensing-based control architecture in multi-fingered arm for object manipulation*", Engineering Letters, vol. 16, issue 2, pp 236 -247, 2008.

[12] C. Cipriani, M. Controzzi, M. C. Carrozza, *The Smart Hand Transradial Prosthesis*, Journal Of Neuro-engineering And Rehabilitation, 2011, n. 8.

[13] V. Ionescu, and A. Zafiu, *Rapid Prosthesis Design Based on Movement Decomposition*, IAENG International Journal of Computer Science, vol 37, issue 1, pp 93-98, 2010.

[14] Rossi C., Savino S., "M*echanical Model of a Single Tendon Finger*", Proc. of ICNAAM 2013: 11th International Conference of Numerical Analysis and Applied Mathematics, Rhodes, Greece, Sep 21-27, 2013

[15] Rossi C., Savino S, "*An underactuated multi-finger grasping device*", International Journal of Advanced Robotic Systems, Volume 11, Issue 1, 17 February 2014, Article number 20.

[16] Rossi C., Savino S., Niola V., Troncone S. (2014) "*A Study of a Robotic Hand with Tendon Driven Fingers*", ROBOTICA. ISSN: 0263-5747, DOI: 10.1017/S0263574714001179.

[17] F. Penta, C. Rossi, S. Savino (2014) *An Underactuated Finger for a Robotic Hand*. International Journal of Mechanics and Control, Vol. 15, n.2, ISSN: 1590-8844.

Maria Karelina was born in Moscow , USSR , on 6 th of June 1966. She received the M.Sc. degree in Technical Sciences (towing and coupling qualities of a tractor gang) in 1992 from the Moscow Automechanic Institute, and the PhD degree in Pedagogics with specialization in humanitarian training of students, in 2000 from the Moscow Sholokhov Pedagogical University. She is the vice-rector for educational work at the Moscow State Technical Automobile and Road University and head of chair "Machinery details and theory of mechanisms". In addition to her valuable research contributions and numerous publications in the area of power plant efficiency and surface-active substances , her current scientific interests include some research in gear durability and robotics.

Eduard Krylov (born in Izhevsk, Russia, 14-th of April 1966) graduated from Moscow Aviation Institute in 1989 and received PhD degree in Mechanics in 1993 from the same institution. He is Associated Professor at the Kalashnikov Izhevsk State Technical University, Department of Theory of Machines. His research interests include analysis of dynamical behavior of machinery, vibration signal processing procedures, thermodynamics, renewable sources of heat energy. Since 2014 Dr. Krylov is a member of IFToMM Permanent Commission for Education.

Cesare Rossi was born in Naples, Italy on 26 July 1955. Graduated at High School focusing on Humanities.
1979 Mechanical Engineer Degree cum Laude at the University of Napoli - “Federico II”.
Technical manager of a textile industry and later designer of tools for aircraft’s tests and maintenance at an aerospace industry.
From 2000 Full Professor of Mechanics for Machines and Mechanical Systems.
Presently teaches Mechanics Fundamentals and Robot Mechanics both to Mechanical and Automation Engineering students. Supervisor of Master and Ph.D. theses and professor at the Ph.D. coursed at the same University.
Research activities where carried on Tribology, Rotor Dynamics, Mechanical Vibrations, Chaotic Motions of Mechanical Systems, Robot Mechanics, Video Applications for Robotics, History of Mechanism and Machine Science. Chair of IFToMM Italy. Member of the IFToMM Permanent Commission for History of Machines and Mechanisms Science (MMS); of the Presidence Board of the Italian Group of Mechanics for Machines and Mechanical Systems; of the Presidence Board of the Department of Industrial Engineering of the University of Naples “Federico II”.

Sergio Savino was born in Naples, Italy, on 7th of May 1975. He received the M.Sc. degree in Mechanical Engineering in 2001, and the PhD degree in Thermomechanical System Engineering with specialization in applied mechanics and robotics, in 2005, both from the University of Naples “Federico II”.
He is a research fellow at the Department of Industrial Engineering, University of Naples “Federico II”. In addition to his valuable research contributions and publications in the area of robotics and computer vision, his current research interests include some investigations in mechanics, in particular in the identification of the objects’ inertia parameters and in analysis of anomalies in gears by means of a wavelet-based signal processing procedure. He has also applied for patents on the following topics: "Robot to scan and replicate surfaces" and "Hand prosthesis in which the five fingers are all driven by a single tie rod inelastic".

F. Timpone (Naples, 5th of September 1974) received the M.Sc. degree in Mechanical Engineering in 1999 and the Ph.D. degree in Thermomechanical System Engineering in 2004 both from the University of Naples “Federico II”. He is Assistant Professor at the University of Naples “Federico II” and his research interests include the dynamics and the control of mechanical systems.
Dr. Timpone became a Member (M) of IAENG in 2015.